Supplementary Information

Unveiling the role of a trinuclear copper(II) cluster in bifunctional OER and HER electrocatalysis: insights from experiment and theory

Sujan Sk,[a] Trishna Ghosh,[a] Aditi De,[b] Julia Klak,[c] Yutaka Hitomi,[d] Subrata Kundu*,[b] and Manindranath Bera*[a]

[a]Department of Chemistry, University of Kalyani, Nadia, West Bengal-741235, INDIA. [b]Process Engineering (EPE) Division, Central Electrochemical Research Institute, Karaikudi-630006, Tamil Nadu, INDIA, and Academy of Scientific and Innovative Research (AcSIR), Ghaziabad-201002, INDIA.

[c]Faculty of Chemistry, University of Wroclaw, Wroclaw 50383, POLAND.

[d]Department of Applied Chemistry, Doshisha University, 1-3 Tatara Miyakodani, Kyotanabe, Kyoto 610-0394, JAPAN.

Figures with Captions

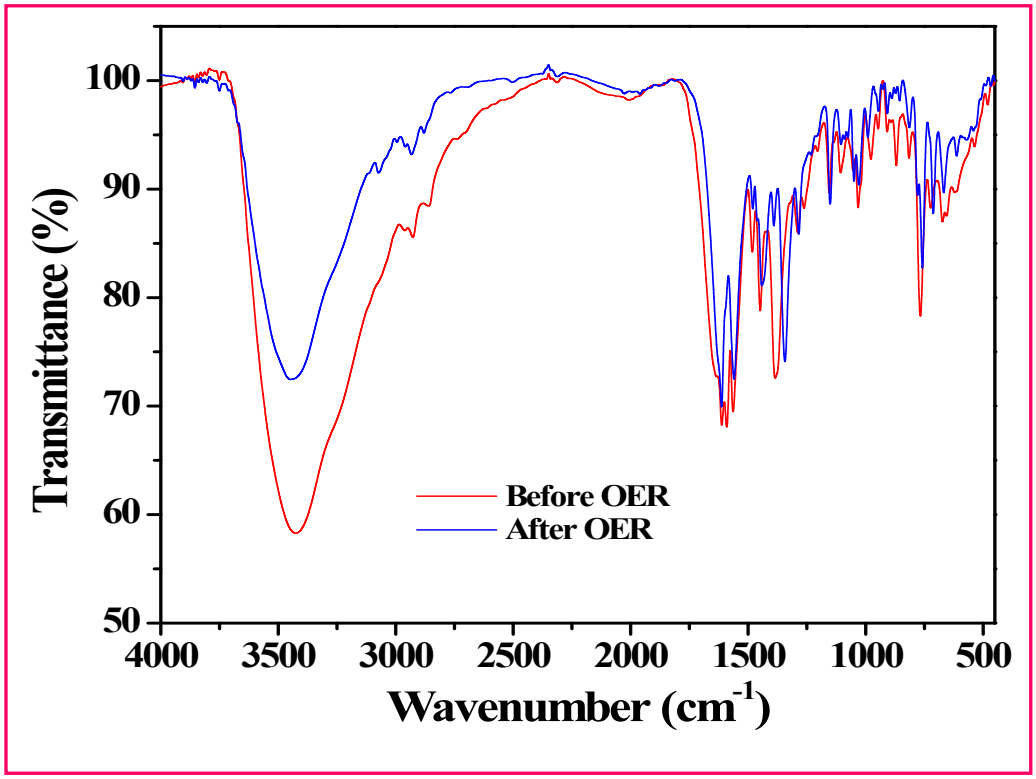

Fig. S1 FTIR spectra of $[Cu_3(L)(OAc)(Cl)_2]\cdot 3H_2O$ before (–) and after (–) OER studies in the region of 4000-450 cm^{-1}.

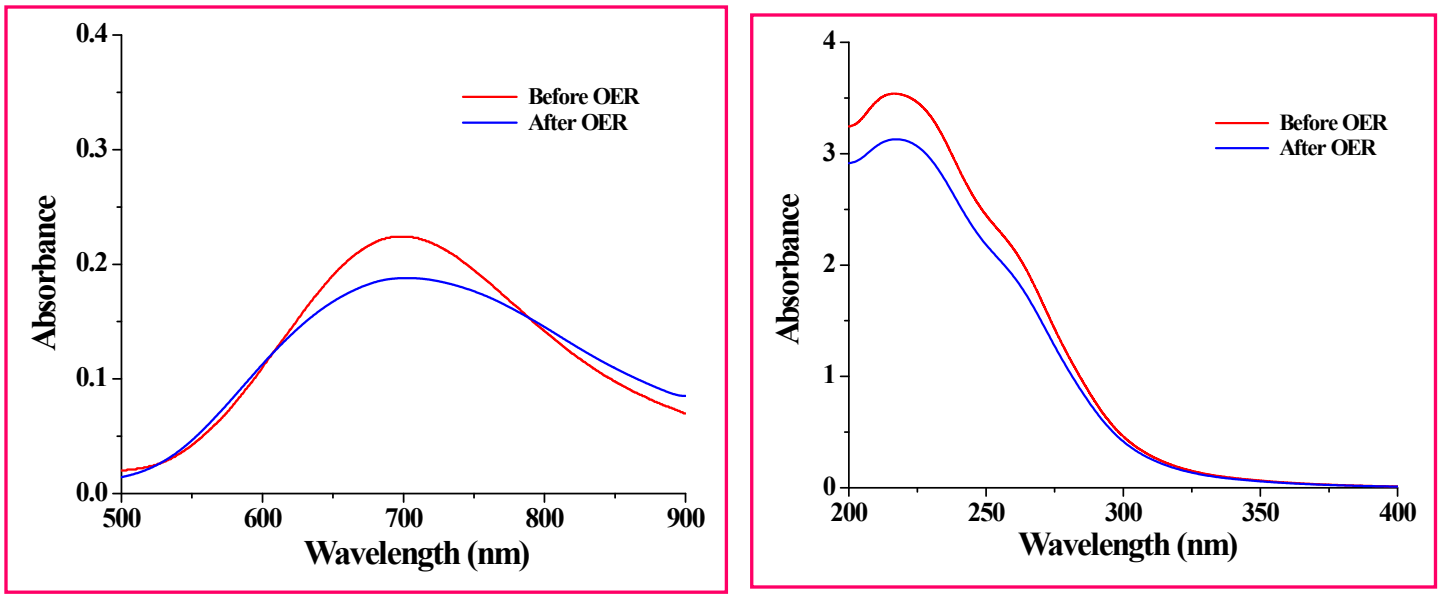

(a) **(b)**

Fig. S2 UV-Vis spectra of $[Cu_3(L)(OAc)(Cl)_2]\cdot 3H_2O$ before (–) and after (–) OER studies with (a) 10^{-3} (M) and (b) 10^{-4} (M) in MeOH solution.

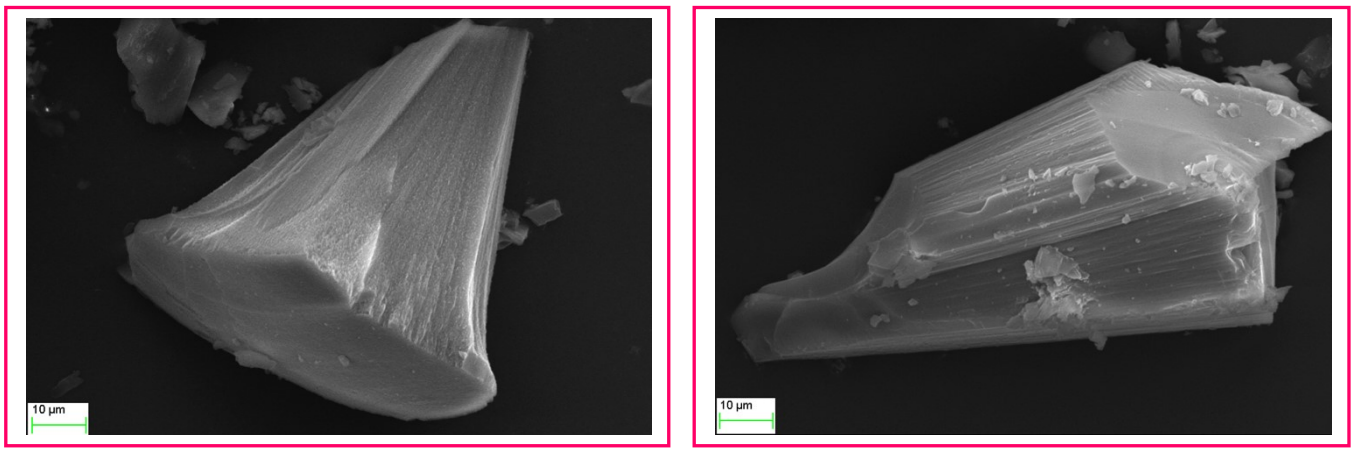

(a) **(b)**

Fig. S3 Scanning electron microscopic (FESEM) images of $[Cu_3(L)(OAc)(Cl)_2]\cdot 3H_2O$ (a) before and (b) after OER studies.

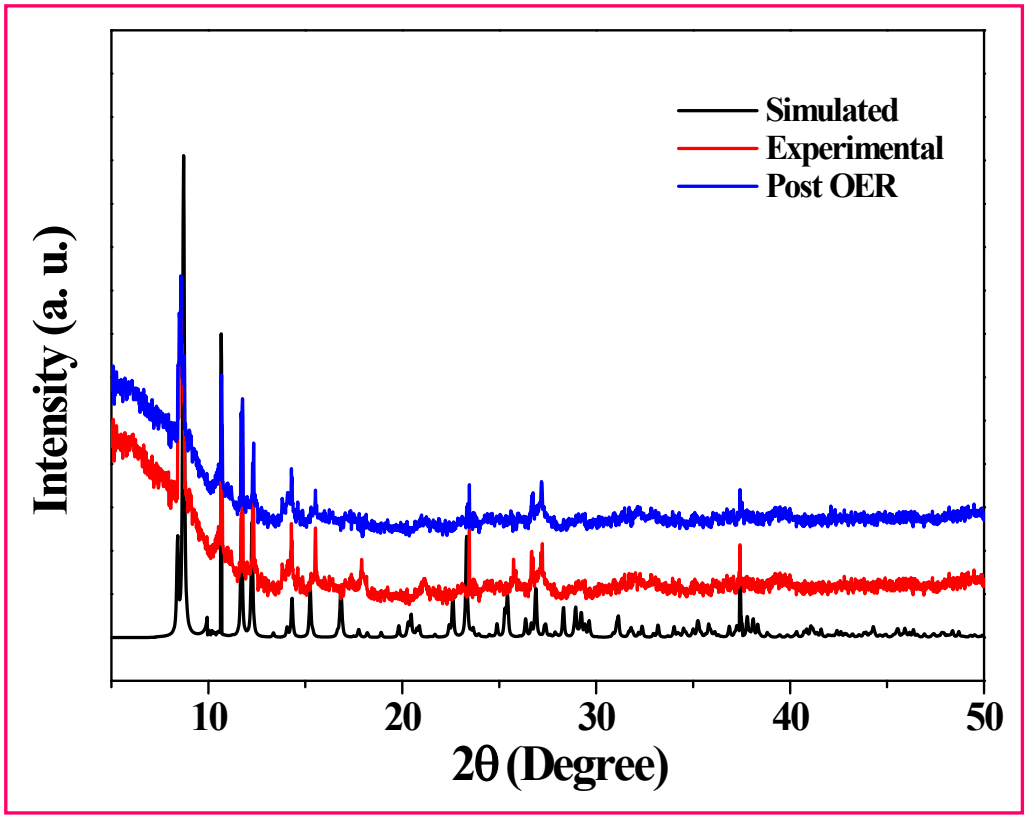

Fig. S4 Powder X-ray diffraction (PXRD) patterns of $[Cu_3(L)(OAc)(Cl)_2]\cdot 3H_2O$: simulated PXRD (–), and experimental PXRD before (–) and after (–) OER studies.

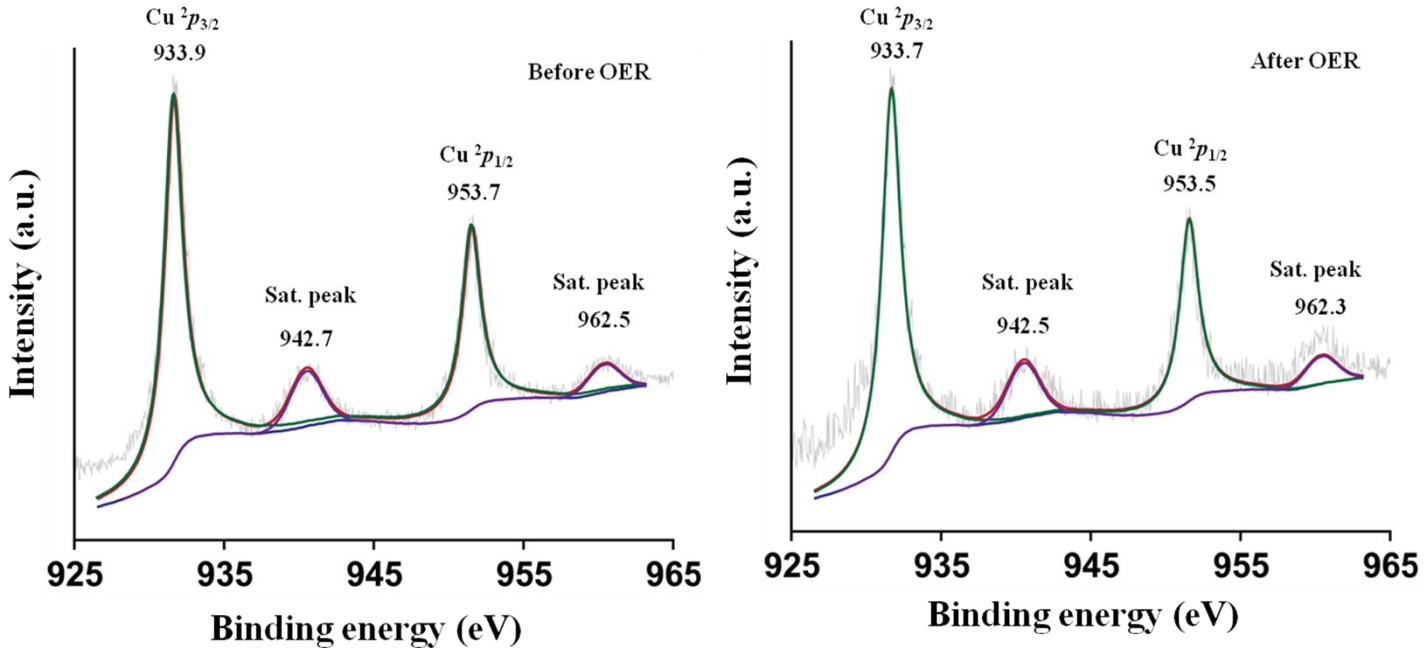

Fig. S5 X-ray photoelectron spectroscopy (XPS) of $[Cu_3(L)(OAc)(Cl)_2]\cdot 3H_2O$ before and after OER studies.

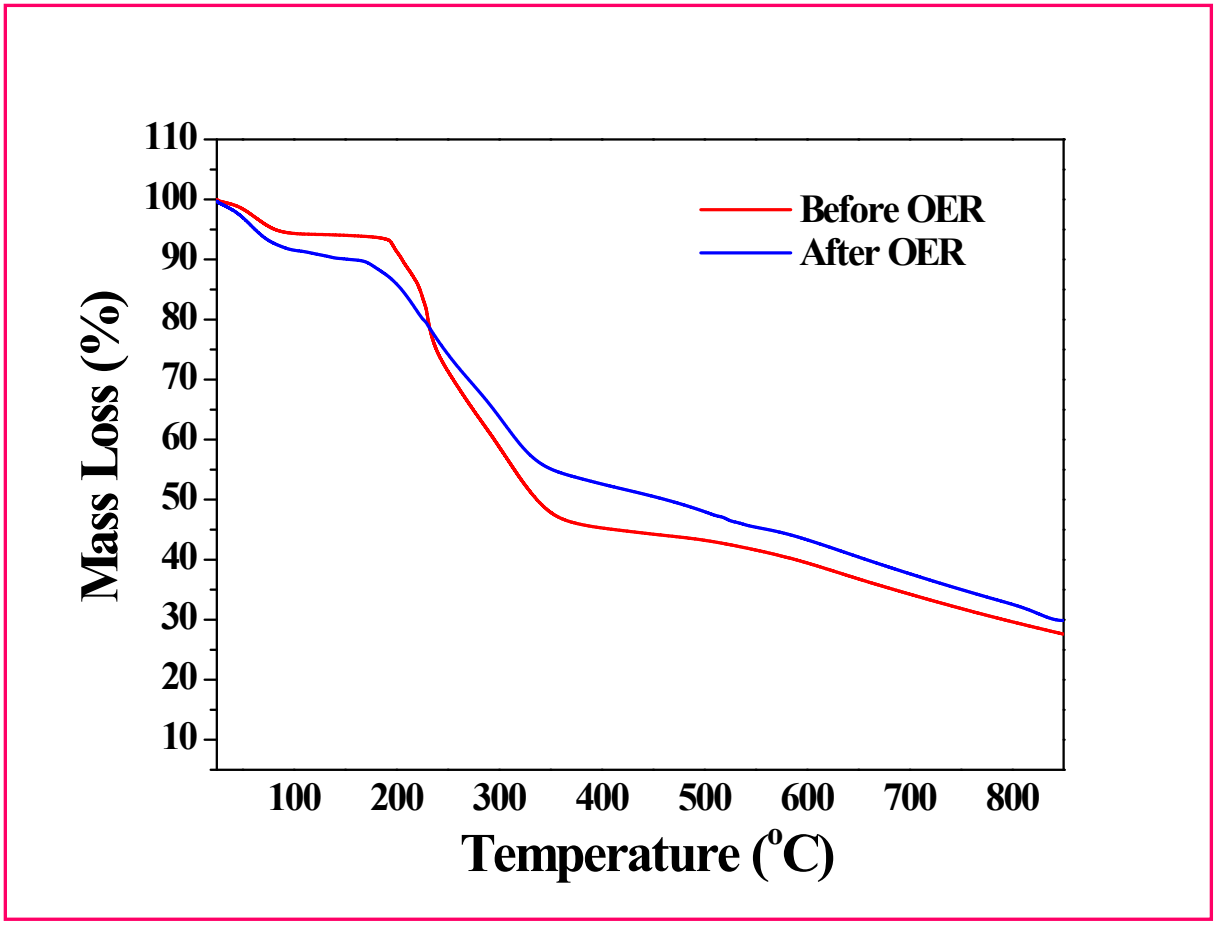

Fig. S6 TGA profiles of $[Cu_3(L)(OAc)(Cl)_2]\cdot 3H_2O$ (a) before and (b) after OER studies under an atmosphere of N_2 gas at a heating rate of ~10°C/min.

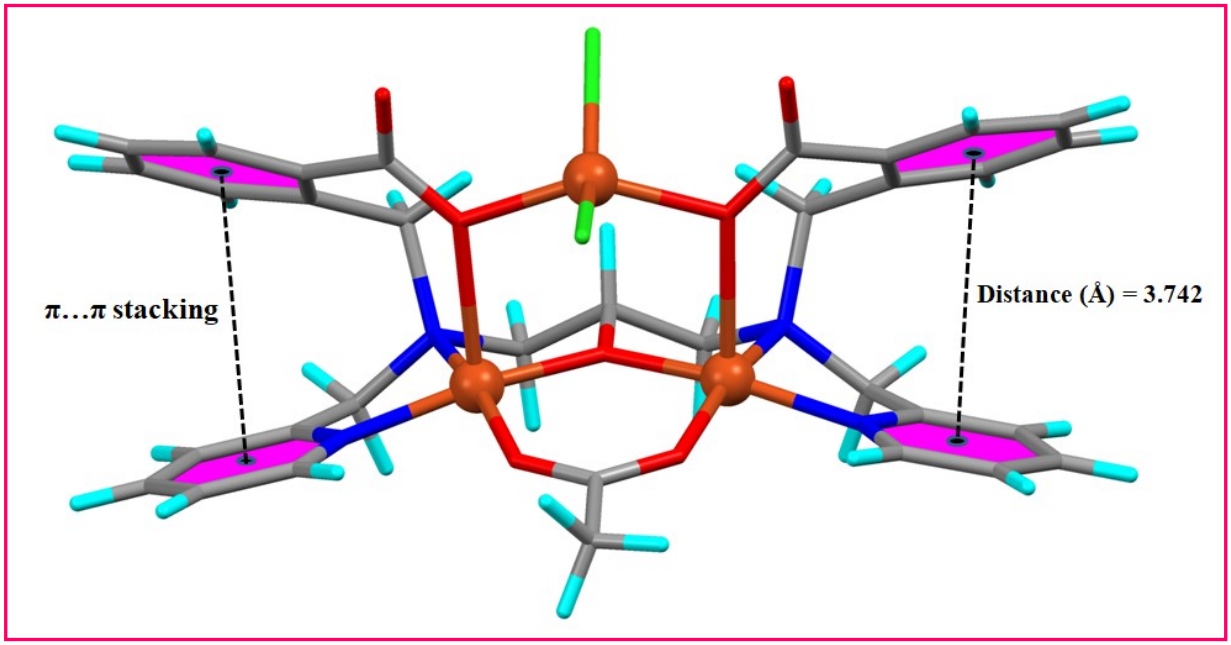

Fig. S7 A view of $[Cu_3(L)(OAc)(Cl)_2]\cdot 3H_2O$ showing intra-molecular π···π stacking interactions.

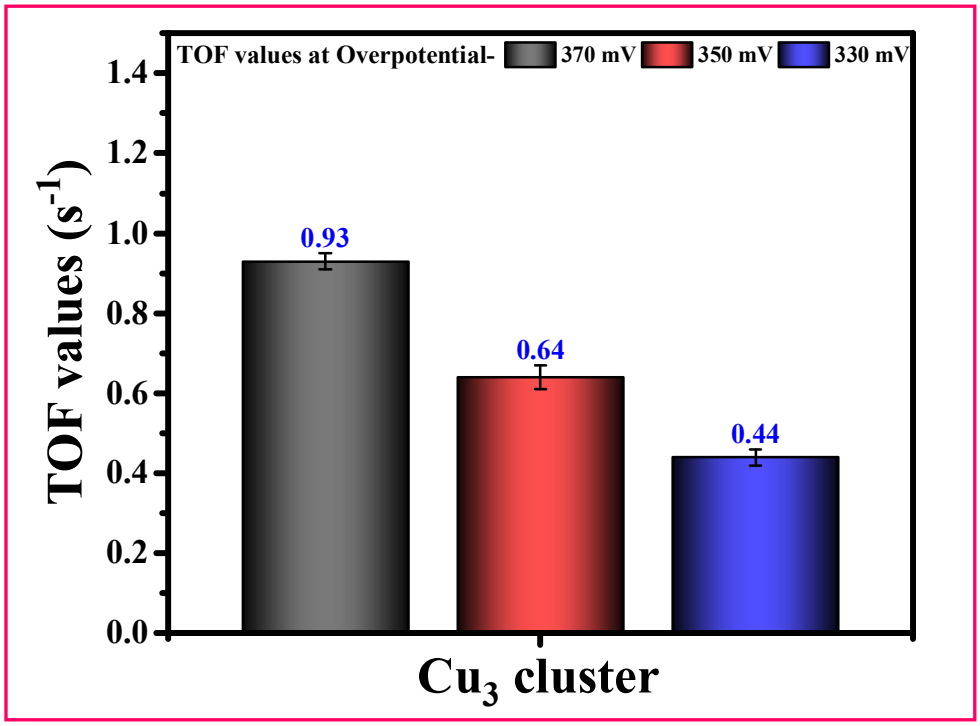

Fig. S8 Bar diagram showing turnover frequency (TOF) values of catalyst $[Cu_3(L)(OAc)(Cl)_2]\cdot 3H_2O$ for OER calculated at various overpotentials (330, 350 and 370 mV).

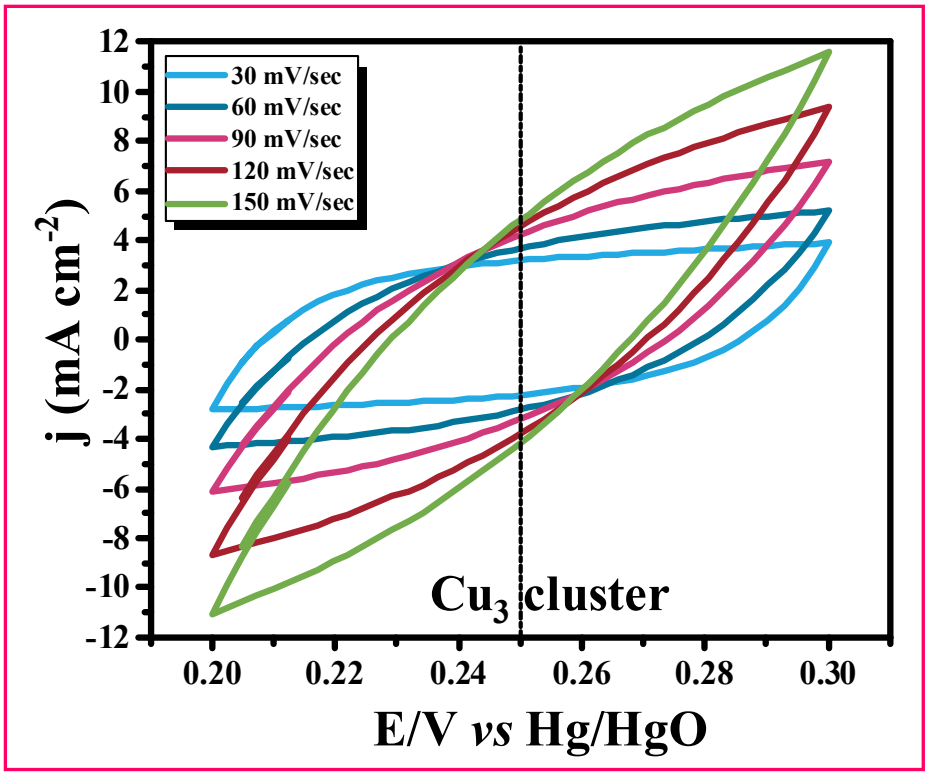

Fig. S9 The CV outcomes of $[Cu_3(L)(OAc)(Cl)_2]\cdot 3H_2O$ for OER studies under the non-Faradaic region at various scan rates.

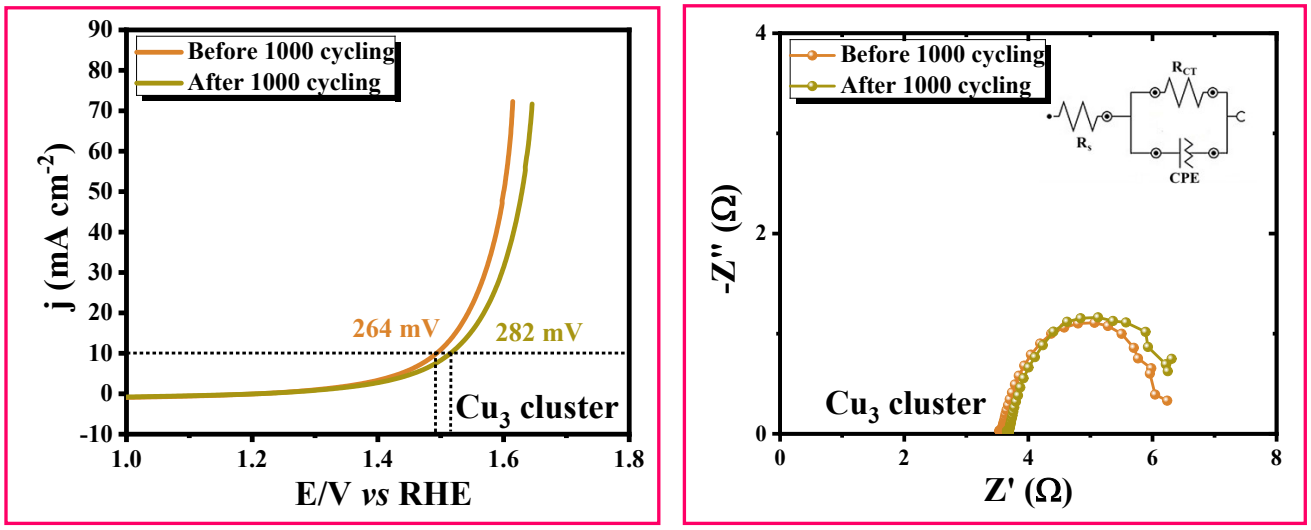

Fig. S10 (a) LSV outcomes, and (b) EIS results of $[Cu_3(L)(OAc)(Cl)_2]\cdot 3H_2O$ before and after the OER-AD studies.

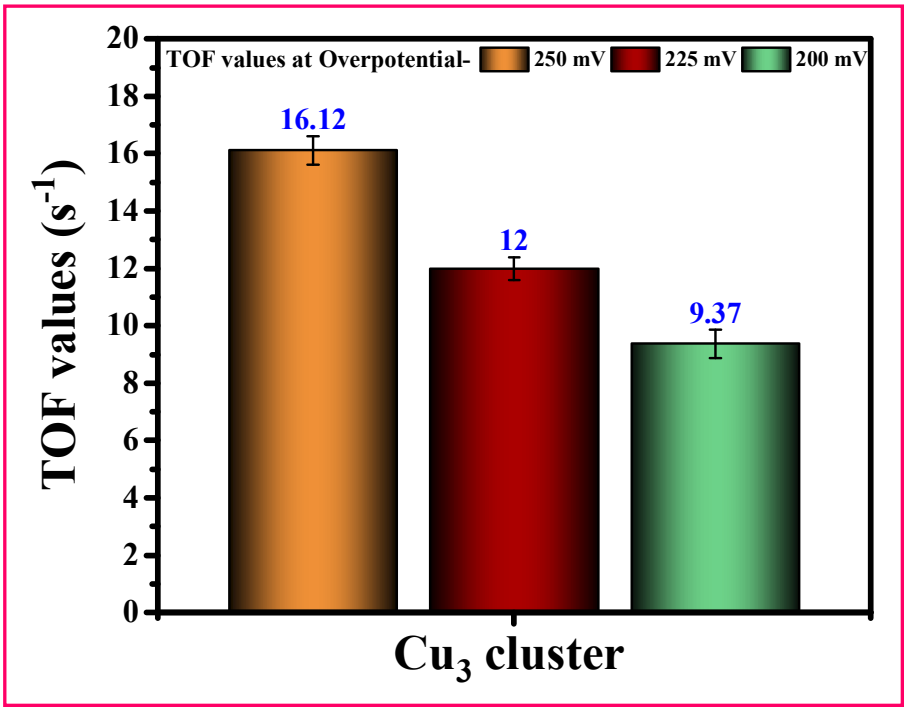

Fig. S11 Bar diagram showing turnover frequency (TOF) values of catalyst $[Cu_3(L)(OAc)(Cl)_2]\cdot 3H_2O$ for HER calculated at various overpotentials (200, 225 and 250 mV).

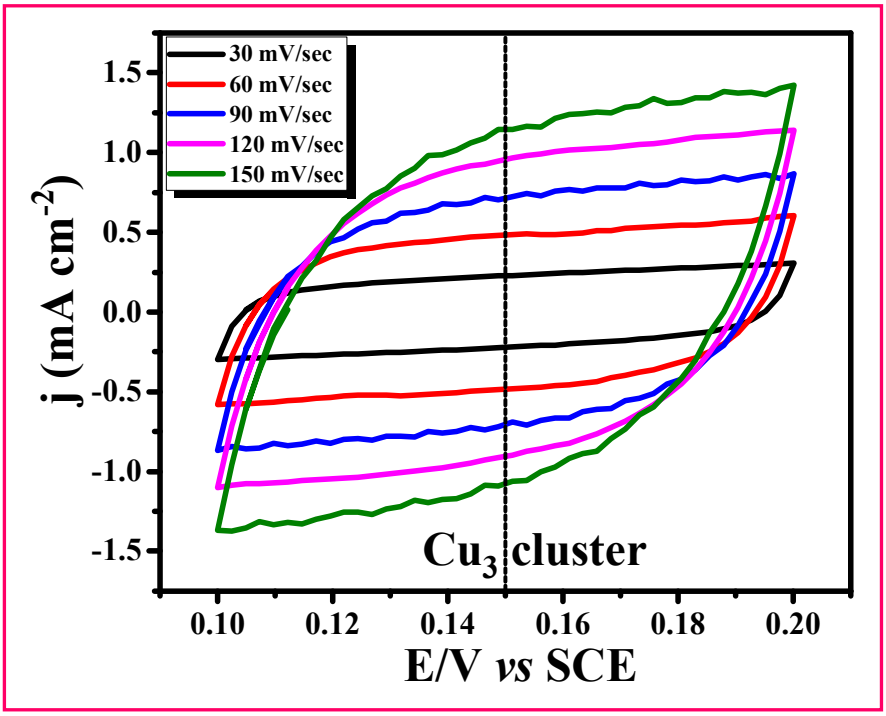

Fig. S12 CV outcomes of $[Cu_3(L)(OAc)(Cl)_2]\cdot 3H_2O$ for HER studies under the non-Faradaic region at various scan rates.

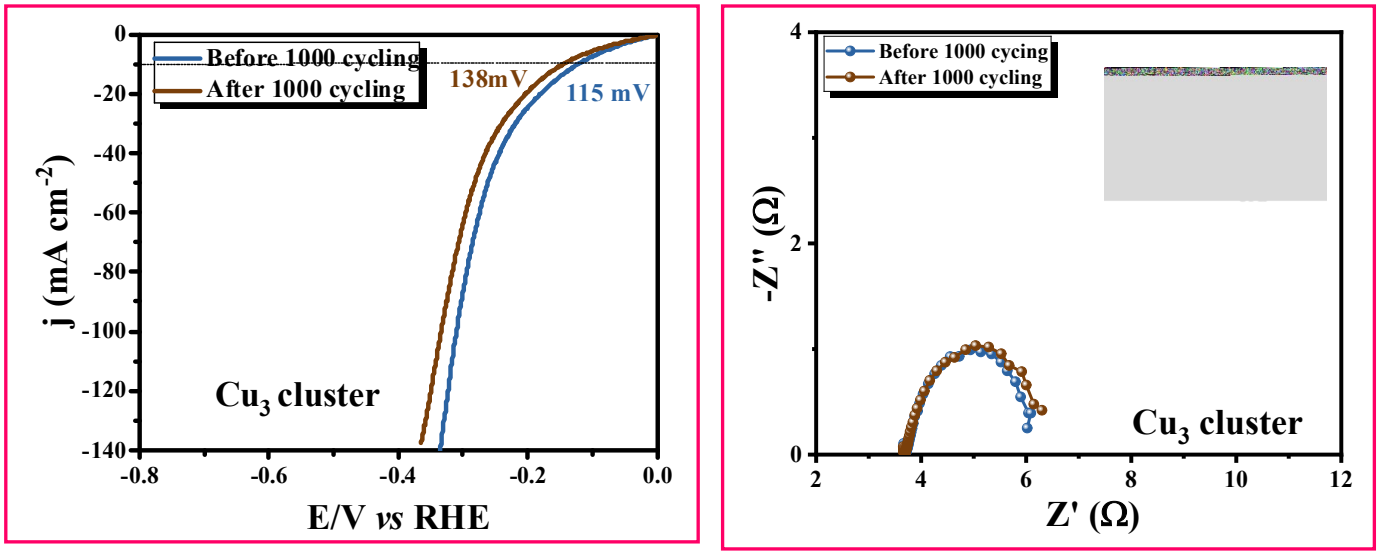

(a) **(b)**

Fig. S13 (a) LSV outcomes and (b) EIS results of $[Cu_3(L)(OAc)(Cl)_2]\cdot 3H_2O$ before and after the HER-AD studies.

Tables with Captions

Table S1 X-ray crystallographic data and parameters for $[Cu_3(L)(\mu\text{-}OAc)Cl_2]\cdot 3H_2O$

	$[Cu_3(L)(\mu\text{-}OAc)Cl_2]\cdot 3H_2O$
Empirical formula	$C_{33}H_{38}N_4O_{10}Cl_2Cu_3$
Formula weight	912.22
Crystal system	Orthorhombic
Space group	*Pnma*
a, Å	17.22(14)
b, Å	15.72(11)
c, Å	13.25(10)
α, deg	90
β, deg	90
γ, deg	90
V, Å^3	3587(47)
Z	4
ρ, Mg/m^3	1.678
Wavelength, Å	0.71073
Temperature, K	302(2)
F(000)	1836
μ, mm^{-1}	1.973
θ range, deg	1.735 to 24.895
Reflections collected	3415
Independent reflections	1956
R(*F*obsd data) [$I > 2\sigma(I)$]	0.0745
wR(F^2 all data)	0.1690
Goodness-of-fit on F^2	1.089
Largest diff. peak and hole, e/Å^3	+ 1.511 to -0.719

$wR2 = \{\Sigma [w(F_o^2 - F_c^2)^2] / \Sigma [w(F_o^2)^2]\}^{1/2}$; $R1 = \Sigma ||F_o| - |F_c|| / \Sigma |F_o|$

Table S2 Selected bond distances (Å) and angles (deg) for $[Cu_3(L)(\mu\text{-}OAc)Cl_2]\cdot 3H_2O$

Bond distances (Å)			
Cu(1)-O(1)	1.834(13)	Cu(2)-N(1)	2.124(16)
Cu(1)-Cl(7)	2.384(18)	Cu(2)-N(2)	1.822(14)
Cu(1)-Cl(8)	2.346(14)	Cu(2)-O(3)	1.780(11)
Cu(2)-O(1)	2.316(15)	Cu(2)-O(2)	2.007(13)
Bond angles (deg)			
O(1)-Cu(1)-O(1')	135.2(6)	O(3)-Cu(2)-N(2)	161.90(4)
O(1)-Cu(1)-Cl(7)	100.9(3)	N(1)-Cu(2)-N(2)	86.50(4)
O(1')-Cu(1)-Cl(7)	100.9(3)	O(3)-Cu(2)-N(1)	80.60(5)
O(1)-Cu(1)-Cl(8)	91.40(3)	O(2)-Cu(2)-N(2)	89.90(4)
O(1')-Cu(1)-Cl(8)	91.40(3)	O(2)-Cu(2)-N(1)	169.30(3)
O(1)-Cu(2)-O(2)	94.00(6)	O(2)-Cu(2)-O(3)	100.50(5)
O(1)-Cu(2)-O(3)	92.40(4)	O(1)-Cu(2)-N(2)	101.70(4)
O(1)-Cu(2)-N(1)	96.60(6)		

Table S3 TOF calculation for catalyst $[Cu_3(L)(OAc)(Cl)_2]\cdot 3H_2O$ for OER

Scan Rate (V/s)	Surface Area (VA)	Associated Charge (C)	F (C/mol)	n	No. of Electron Transfer	J (A/cm^2)	N_A	$J \times N_A$	$(n \times F \times \tau)$	TOF (s^{-1})	Measured at Potential *vs.* RHE (V)	Over-potential (mV)
0.03	0.000419	0.013967	96485	4	8.7183×10^{16}	0.025	6.023×10^{23}	1.5×10^{22}	3.36×10^{22}	0.448	1.56	330
0.03	0.000419	0.013967	96485	4	8.7183×10^{16}	0.036	6.023×10^{23}	2.2×10^{22}	3.36×10^{22}	0.644	1.58	350
0.03	0.000419	0.013967	96485	4	8.7183×10^{16}	0.052	6.023×10^{23}	3.1×10^{22}	3.36×10^{22}	0.930	1.60	370

Table S4 The electrochemical kinetic, activity and OER performance-based parameters of catalyst $[Cu_3(L)(OAc)(Cl)_2]\cdot 3H_2O$

Parameters	Cu_3 catalyst	RuO_2
EIS R_{ct} (Ω)	2.72	6.57
EIS R_s (Ω)	3.48	6.12
ECSA (cm^2)	373.75	-
Overpotential @ 10 mA/cm^2 (mV)	1.494 V (264 mV)	1.491 V (370 mV)
Overpotential @ 20 mA/cm^2 (mV)	1.543 V (313 mV)	1.63 V (400 mV)
Overpotential @ 30 mA/cm^2 (mV)	1.57 V (340 mV)	1.65 V (420 mV)
C_{dl} (mF/cm^2)	14.945	-
Mass loading (mg)	1.1	-
Tafel slope (mV/dec)	65.01	76.85

Table S5 TOF calculation of catalyst $[Cu_3(L)(OAc)(Cl)_2]\cdot 3H_2O$ for HER

Scan Rate (V/s)	Surface Area (VA)	Associated Charge (C)	F (C/mol)	n	No of Electrons Transfer	J (A/cm^2)	N_A	$J \times N_A$	$(n \times F \times \tau)$	TOF (s^{-1})	Measured at Potential *vs.* RHE (V)	Over-potential (mV)
0.03	0.00004	0.001333	96485	2	8.32×10^{15}	0.025	6.023×10^{23}	1.5×10^{22}	1.6×10^{21}	9.375	0.200	200
0.03	0.00004	0.001333	96485	2	8.32×10^{15}	0.032	6.023×10^{23}	1.9×10^{22}	1.6×10^{21}	12.000	0.225	225
0.03	0.00004	0.001333	96485	2	8.32×10^{15}	0.043	6.023×10^{23}	2.6×10^{22}	1.6×10^{21}	16.126	0.250	250

Table S6 The electrochemical kinetic, activity and HER performance-based parameters of catalyst $[Cu_3(L)(OAc)(Cl)_2]\cdot 3H_2O$

Parameters	Cu_3 catalyst	Pt/C
EIS R_{ct} (Ω)	2.46	0.97
EIS R_s (Ω)	3.66	1.27
ECSA (cm^2)	183.75	-
Overpotential @ 10 mA/cm^2 (mV)	-0.115 V (115 mV)	-0.036 V (36 mV)
Overpotential @ 20 mA/cm^2 (mV)	-0.181 V (181 mV)	-0.058 V (58 mV)
Overpotential @ 30 mA/cm^2 (mV)	-0.219 V (219 mV)	-0.066 V (66 mV)
C_{dl} (mF/cm^2)	7.35	-
Mass loading (mg)	1.1	-
Tafel slope (mV/dec)	42.45	32.97

Table S7 Energies of the different intermediate species with a schematic diagram observed during the OER process computed by DFT method

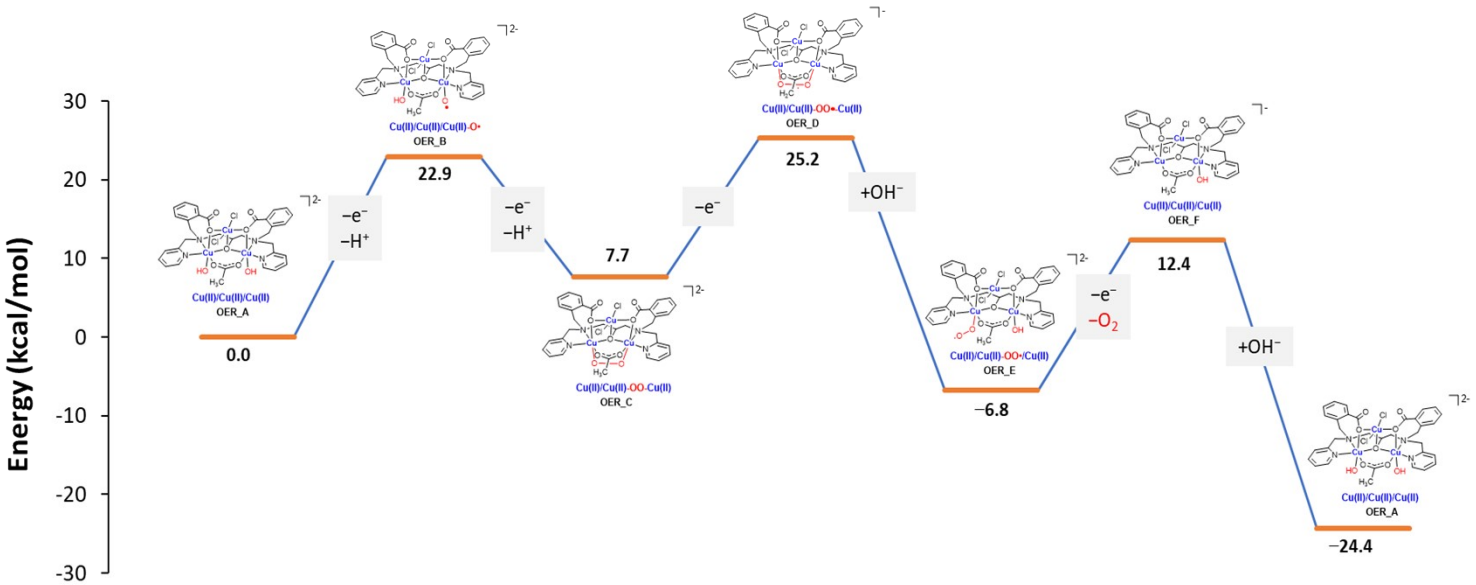

Species	Energy/Hartree	Energy/kcal mol^{-1}
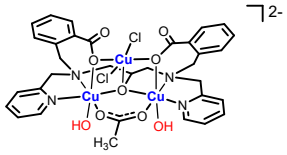 Cu(II)/Cu(II)/Cu(II) OER_A	-8012.90684634	-5028179.175
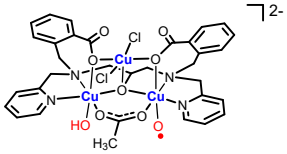 Cu(II)/Cu(II)/Cu(II)-O• OER_B	-8012.23735028	-5027759.06
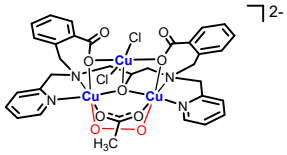 Cu(II)/Cu(II)-OO-Cu(II) OER_C	-8011.62865274	-5027377.096
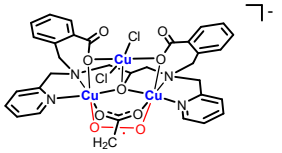 Cu(II)/Cu(II)-OO•-Cu(II) OER_D	-8011.50962433	-5027302.404
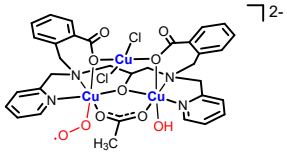 Cu(II)/Cu(II)-OO•/Cu(II) OER_E	-8087.34614147	-5074890.577
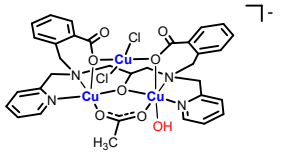 Cu(II)/Cu(II)/Cu(II) OER_F	-7937.062902	-4980586.341

Table S8 Energies of the different intermediate species with a schematic diagram observed during the HER process computed by DFT method

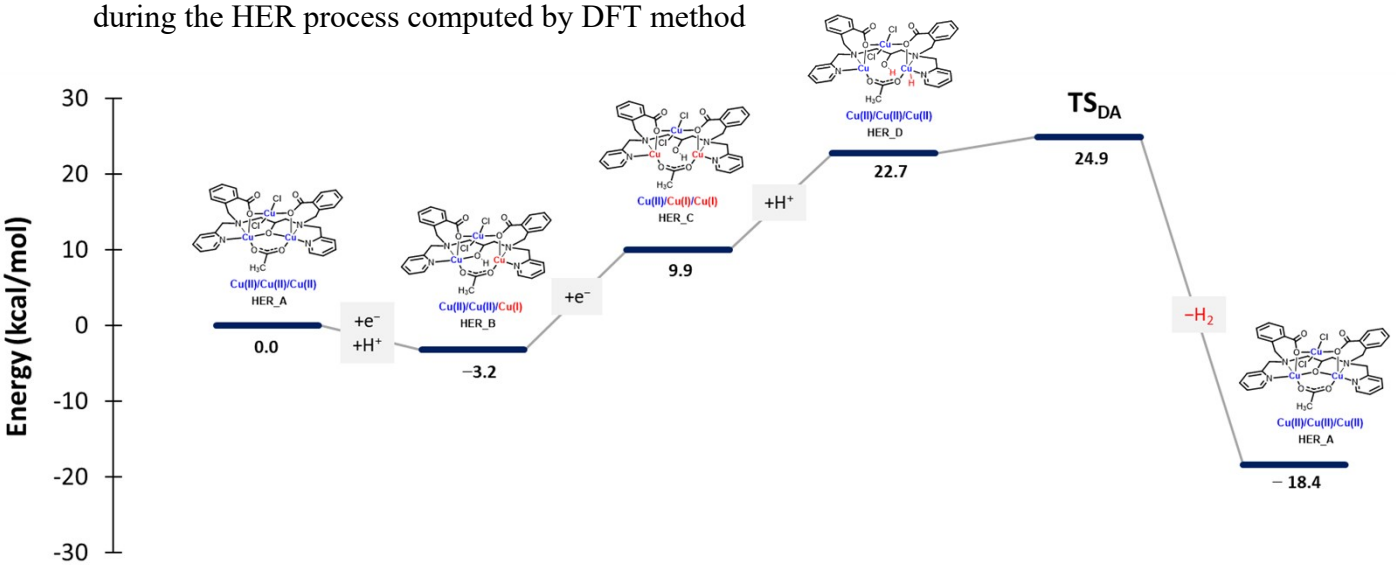

Species	Energy/Hartree	Energy/kcal mol^{-1}
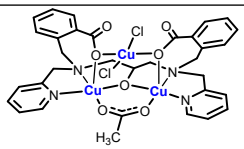 Cu(II)/Cu(II)/Cu(II) HER_A	-7861.221237	-4932994.938

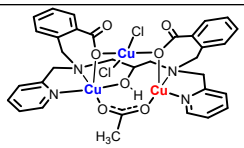 Cu(II)/Cu(II)/Cu(I) HER_B	-7861.796231	-4933355.753
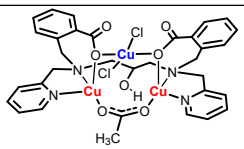 Cu(II)/Cu(I)/Cu(I) HER_C	-7861.938761	-4933445.192
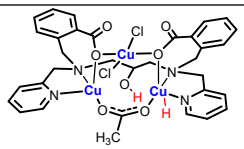 Cu(II)/Cu(II)/Cu(II) HER_D	-7862.324784	-4933687.425

Determination of Turnover Frequency (TOF), Surface Concentration, Surface Charge of the Cu_3 Catalyst for OER from C_{dl}-Derived CV Curve at a Low Scan Rate of 30 mV s^{-1}:

Calculated integrated area acquired from C_{dl}-derived CV curve at a low scan rate of 30 mV s^{-1} = 0.000419 VAcm^{-2}

Hence, the associated surface charge (Q) = 0.000419 VAcm^{-2} / 30 mVs^{-1}

= 0.013967 Ascm^{-2}

= **0. 013967 C cm^{-2}**

Now, the number of electrons transferred = 0.013967 C cm^{-2} / 1.602 ×10^{-19} C

= **8.71 × 10^{16} cm^{-2}** (electrode area 1*1 cm^2)

The corresponding expression to determine the Turnover Frequency (TOF) from OER current density is,

$$TOF = \frac{j \times N_A}{n \times F \times \tau} \quad \text{..... (S1)}$$

where, j = current density, N_A = Avogadro number, F = Faraday constant, n = number of electrons for OER = 4, Γ = surface concentration.

Hence, we have,

$TOF_{\Gamma(CV)@370\ mV}$ = [(0.052) Acm^{-2} $(6.023\times 10^{23)}$] mol^{-1} / [(96485) $Cmol^{-1}$ (4) (8.71×10^{16}) cm^{-2}]

= **0.930 sec^{-1}**

Determination of Turnover Frequency (TOF), Surface Concentration, Surface Charge of the Cu_3 Catalyst for HER from C_{dl}-Derived CV Curve at a Low Scan Rate of 30 mV s^{-1}:

Calculated integrated area acquired from C_{dl}-derived CV curve at a low scan rate of 30 mV s^{-1} = 0.00004 $VAcm^{-2}$

Hence, the associated surface charge (Q) = 0.00004 $VAcm^{-2}$ / 30 mVs^{-1}

= 0.0013333 $Ascm^{-2}$

= **0. 0013333 C cm^{-2}**

Now, the number of electrons transferred = 0.0013333 C cm^{-2} / 1.602 $\times 10^{-19}$ C

= **8.32×10^{15} cm^{-2}** (electrode area 1*1 cm^2)

The corresponding expression to determine the Turnover Frequency (TOF) from OER current density is,

$$TOF = \frac{j \times N_A}{n \times F \times \Gamma} \quad \text{..... (S1)}$$

where, j = current density, N_A = Avogadro number, F = Faraday constant, n = number of electrons for HER = 2, Γ = surface concentration.

Hence, we have,

$TOF_{\Gamma(CV)@250\ mV}$ = [(0.043) Acm^{-2} $(6.023\times 10^{23)}$] mol^{-1} / [(96485) $Cmol^{-1}$ (4) (8.32×10^{15}) cm^{-2}]

= **16.12 sec^{-1}**